J. Inst. Eng. India Ser. C (August 2021) 102(4):995–1005
https://doi.org/10.1007/s40032-021-00709-4

ORIGINAL CONTRIBUTION

Numerical Investigation of a Hydro-cyclone for Separating Organic and Aqueous Phases

Saeed Raeesi[1] · Ataallah Soltani Goharrizi[1] · Bahador Abolpour[2]

Received: 18 September 2020 / Accepted: 28 April 2021 / Published online: 3 June 2021

Abstract The separation of fluid–fluid mixtures is one of the main problems in different industries. Due to the high efficiency of liquid–liquid hydro-cyclone in the separation of fluid mixtures and its easy installation and reasonable prices, this device has a width application in these industries. In this study, a three-dimensional simulation has been presented to evaluate these hydro-cyclones performances. Because of the presence of a high swirling fluid flow, the Reynolds stress model has been utilized to model this turbulent flow. The mixture model has been utilized to simulate the multiphase flow within the hydro-cyclone. The efficiency of the hydro-cyclone separation has been validated using the results of experimental data. The influence of hydro-cyclone geometry and also operational parameters have been investigated.

Keywords Hydro-cyclone · Aqueous-organic mixture separation · Computational fluids dynamics

Introduction

The separation of fluids mixtures is an attractive study for researches and engineers. Today, using of hydro-cyclones is one of the most important methods for separating liquid–liquid two-phase fluids. Variability in application, simple utilization and low structural and operation costs are the benefits of using hydro-cyclones for this purpose. As shown in Fig. 1, the liquid–liquid hydro-cyclone separator has been made from simple components, such as inlet chamber, the section of cylindrical area, reducing and also tapered section, tail pipe and two overflow sections for offloading the phases [1]. Entering the inlet fluid as a tangential flow to the hydro-cyclone wall provides a circulation inside this hydro-cyclone and makes two vortex flows in this two-phase fluid [2]. The first vortex flow leads the heavier phase toward the cyclone wall, and the second vortex flow leads the lighter phase toward the center-line of this cyclone. This is the mechanism of separation of these phases within this hydro-cyclone. The fluid flow pattern and also extend of these vortex flows are depended to the size and shape of the inlet section [3, 4]. The offloading sections obtain the cyclone capacities attending to the inlet light phase fraction or split ratio. The sizes of these sections are depending on the application type of this cyclone [5]. The size and shape of the cylindrical section affect the vortex flow and the split ratio of this cyclone, subsequently [6]. The reducing section increases the fluid flow velocities, increases the strain stress and pressure drop and may cause the breaking down of droplets and decaying the split ratio of the cyclone [1]. The tapered section has important effects on the split ratio by increasing the residence time of the fluid flow with a suitable vorticity [6]. The tail pipe has been located at the end of tapered section to increase the residence time of the fluids [6, 7]. Various structural and coating materials have been used in these hydro-cyclones, which make their walls hydrophobic or oleophobic.

Hargreaves and Silvester [8] studied the water–oil flow inside a hydro-cyclone, numerically, using the Euler-Lagrangian method. The obtained experimental results using the laser velocimetry approved their numerical simulation.

✉ Bahador Abolpour
bahadorabolpor1364@yahoo.com

[1] Department of Chemical Engineering, Shahid Bahonar University of Kerman, Kerman, Iran

[2] Department of Chemical Engineering, Sirjan University of Technology, Sirjan, Iran

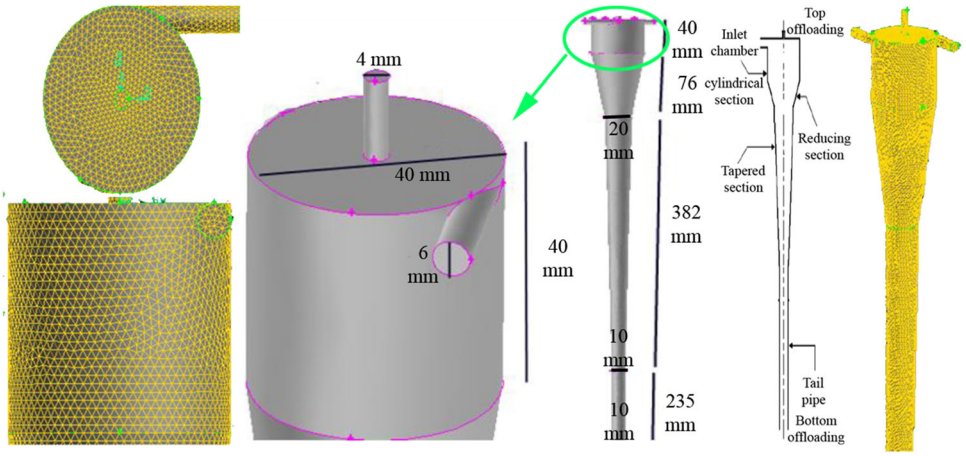

Fig. 1 The configuration of the defined geometry and mesh for the liquid–liquid hydro-cyclone

Young et al. [6] investigated the fluid flow in a liquid–liquid hydro-cyclone. They resulted that the droplets size, densities difference and the dimension of the cylindrical part have important effects on the split ratio of this cyclone. Grady et al. [9] simulated the fluid flow patterns inside an oil separator hydro-cyclone and obtained the velocity profile and also the efficiency of this cyclone. They illustrated that the Reynolds stress model approach is able to simulate the vortex flow within this cyclone, accurately. Petty and Park [10] presented the idea of using very small liquid–liquid hydro-cyclones for oil separation. Their numerical simulation of vortex flow inside these cyclones shows that there is a centrifugal acceleration within these cyclones as more as three times of the gravitational acceleration. Huang [11] presented a three-dimensional simulation for a turbulent flow of water–oil mixture (with a more than 10% of volumetric fraction of desecrated phase) in a hydro-cyclone using the Eulerian–Eulerian and the Reynolds stress modeling viewpoint. He approved the predictions of this numerical model using the experimental data. Kharoua et al. [12] investigated the oil separation and also predicted the velocity profiles which includes axial and tangential velocity components in a hydro-cyclone using the Reynolds stress and $k-\varepsilon$ turbulent models. They resulted that these hydro-cyclones have a low performance in the oil separation of high concentrations mixtures. Zhao et al. [13] showed that an air injection to the oil separator hydro-cyclone improves the ability of this cyclone for oil separation. Teja et al. [14] demonstrated the effects of the slope of the tapered area of this hydro-cyclone on its performance, numerically and experimentally. Jiawang et al. [15] presented a numerical design for the water–oil separator hydro-cyclone. They obtained an optimum pressure drop in a high-performance cyclone. Osei et al. [16] used the computational fluids dynamic for investigating the cylindrical section length effect and also the inlet section on the split ratio of the cyclone. Fan [17] used a similar method for investigating the effects of the operating conditions and also the properties of inlet mixture on this ratio. Qian et al. [18] investigated the influence of the slope of the tapered section and also the inlet fluid flow on the droplet concentration within a liquid–liquid hydro-cyclone. Motin and Benard [19] also investigated the effects of the geometry of the circulation section of the hydro-cyclone on its split ratio.

Delgadillo and Rajamani [27] compared three different models of $k-\varepsilon$ group renormalization, the Reynolds stress and the large eddy simulation (LES), in order to predict air-core dimension, mass split, axial and tangential component of velocity variables in hydro-cyclone. They investigated good agreement of particle tracking by velocity field with experimental size–classification curve. Narasimha et al. [28] simulated the fluid flow through hydro-cyclone by Fluent commercial software package and good agreements have been achieved for the forecasted water splits in the outlet sections for different inlet water amount according to discrete phase modeling technique as first step of process. Additionally, particles classification based on their size has been observed. Delgadillo and Rajamani [29] used Fluent software to investigate desired classification of hydro-cyclone based on hydrodynamics parameters. They used the (LES) approach for simulating turbulence flow and particle-tracking method has been implemented based on the Lagrangian method in order to track particles locations. Six new developed geometries compared with basic geometries in the case of mass balance and classification curve. Chakraborti and Miller [30] presented an acute evaluation of fluid flow models and flow measurement techniques in hydro-cyclones. In their study, empirical, semi-empirical and the equation of Navier–Stokes are discussed.

The transient swirl flow simulation in the hydro-cyclone separators has been done by Chakraborti et al. [31]. They used Fluent package as CFD simulation software. Also, they developed 'novel multi-objective genetic algorithm' in their studies. The volume of the locus of zero vertical velocity (LZV) and the overall pressure drop have been

optimized simultaneously in their model. Delgadillo and Rajamani [32] compared Reynolds stress model (RSM) and $k-\varepsilon$ model with velocity profiles. Their investigation has been done in 75 and 250 mm diameter hydro-cyclones. They observed that the RSM and $k-\varepsilon$ models were not able to estimate velocity profile, and large eddy simulation method has been introduced for velocity profile estimation. Suresh [33] presented the experimental setups for investigating the separation performance characteristics of the dense media hydro-cyclone (DMC). Hsieh and Rajamani [34] developed a new mathematical and theoretical model for hydro-cyclone according to the physical approach of the fluid flow. The velocity profile and separation efficiency curve have been estimated as the output of developed model. They validated their results with laser-doppler velocimeter (LDV) to investigate the velocity values inside a 75-mm hydro-cyclone. In order to illustrate increasing of slurry viscosity, pure water and the mixture of the glycerol-water have been used in the presence of particles. Monredon et al. [35] investigated the stability of developed mathematical model of the hydro-cyclone based on the physics of fluid flow with extreme variation in device geometries. They used five hydro-cyclones, and velocity profiles have been measured by the LDV.

In 2009, Kharoua et al. [36] examined the separation of petroleum from water and predicted axial and tangential velocity components in a hydro-cyclone. In this work, they used the RNG and RSM turbulent models to investigate the effect of mixing on the velocity profiles and the mixed multiphase model for the system in multiphase mode. They investigated the effect of changes in concentration of the oil at the inlet, the size of oil droplets and inlet fluid flow on separation efficiency. Their results showed that, for high oil concentrations, the separation efficiency has been decreased and with increasing the inlet fluid flow, the separation efficiency has been increased. They also resulted that the RSM model has less error with the experimental results, comparing with the RNG model. Cullivan et al. [37] numerically examined the pressure distribution and particle routing. Using the RSM turbulence model, they simulated the air-core inside the hydro-cyclone and found that specifically in this geometry and this flow there is a significant difference between the turbulent RSM model and the turbulent models of the two equations.

- In the present study, the fluid flow patterns have been simulated using the computational fluids dynamic for investigating the effects of different geometrical and operating effective factors, such as the hydrophobic and oleophobic walls of the hydro-cyclone, on the separation performance of the liquid–liquid hydro-cyclone. Finally, a set of cases, with a full factorial experimental design, of different sizes of three dimensions of this hydro-cyclone has been tested in this simulation for obtaining the optimum geometry with a maximum separation performance in this cyclone. This study presents valuable results for designing a suitable hydro-cyclone for separating oil from water. For designing high-efficiency and low-pressure-drop hydro-cyclone for this propose, the wall hydrophobic properties, inlet zones and also flowrate of the mixture fluid, the sizes of top offloading and also the tail pipes, and different sections of the hydro-cyclone section have been optimized in this study. Therefore, the presented ideas in this study can be developed for designing various hydro-cyclones with different operating purposes.

Methodology

First, a three-dimensional geometry of a predesigned cyclone [20] has been defined as the presented geometry in Fig. 1. Then, a nonstructural tetrahedral hybrid grid has been used for meshing within this geometry, as shown in Fig. 1. Inlet constant fluid flow velocity (6 m s^{-1}), uniform outflows (0.17 and 0.83 kg s^{-1} mass flows of the top and

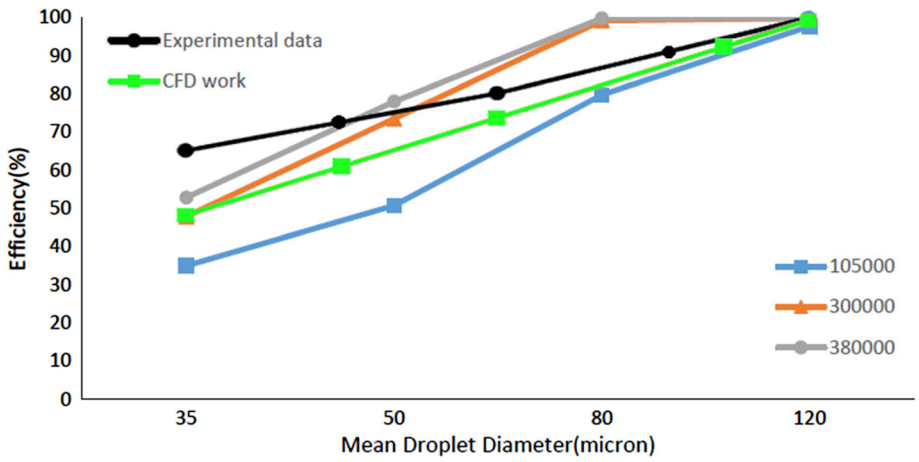

Fig. 2 Mesh study and comparing the model predictions with the experimental data [26]

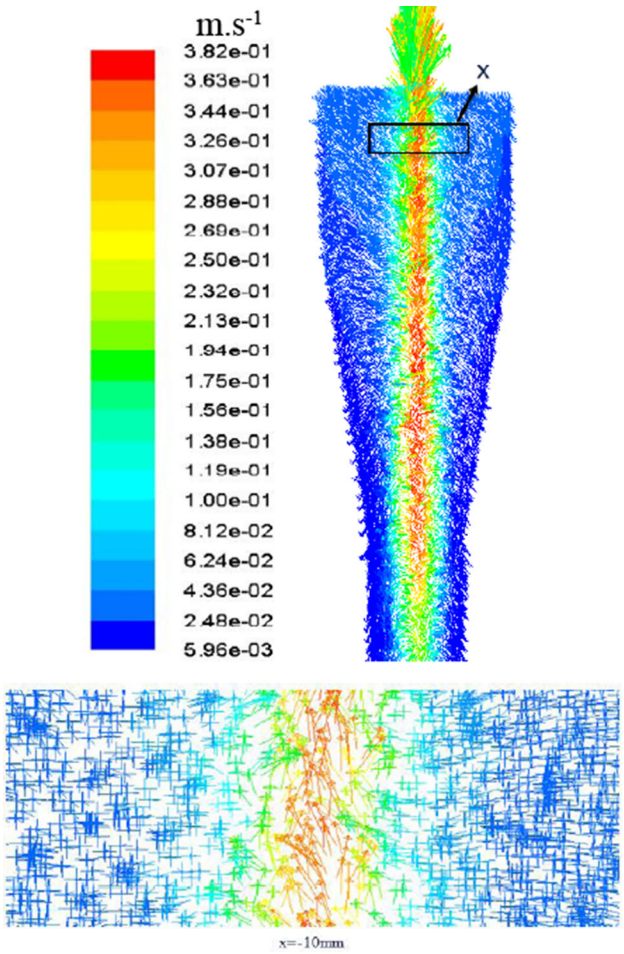

Fig. 3 The fluid flow contour plot inside the cyclone

bottom offloads, respectively) and no-slip are defined boundary conditions for the fluid flow in this cyclone. The properties of inlet mixture have been defined as 95% and 5% volume fractions, 998 and 850 kg m^{-3} densities and 0.001 and 0.0032 kg m^{-1} s^{-1} for the water and oil fluids, respectively.

Attending to the low concentration of oil in the inlet mixture and also low values of the droplet relaxation time (*i.e.*, $\frac{(\rho_m-\rho_p)d_p^2}{18\mu_f} = 1.7 \times 10^{-5}$ that is smaller than 0.001), the mixture model has been considered for this simulation. The continuity equation has been defined as [21]:

$$\frac{\partial}{\partial t}(\rho_m) + \nabla.\left(\rho_m \overrightarrow{v_m}\right) = 0 \quad (1)$$

where t is time, $\overrightarrow{v_m} = \frac{\sum_{k=1}^{n} \alpha_k \rho_k v_k}{\rho_m}$ is the mass averaged velocity of a n-component mixture fluid, $\rho_m = \sum_{k=1}^{n} \alpha_k \rho_k$ is the mean density of this mixture and α_k is the volume fraction of k^{th} phase. The momentum balance equation for a mixture is a summation of the balance of the momentum for each phase, which can be presented as below [21]:

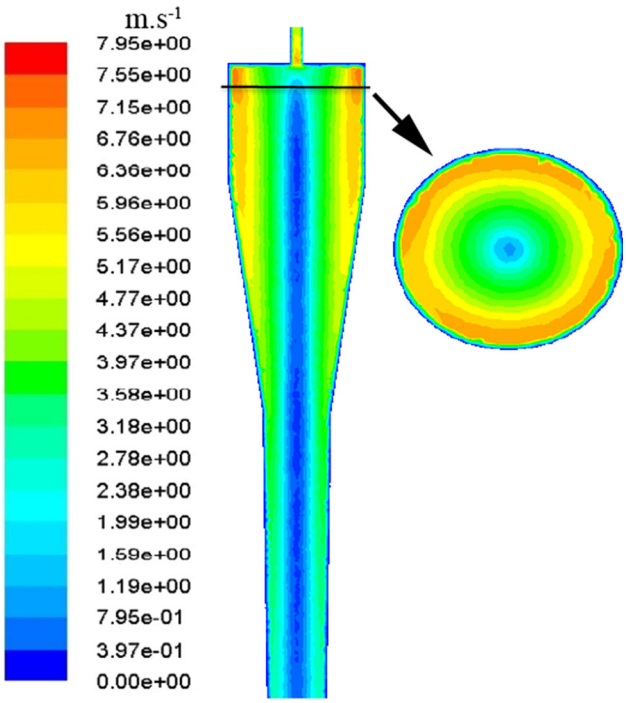

Fig. 4 The velocity of fluid flow inside the cyclone

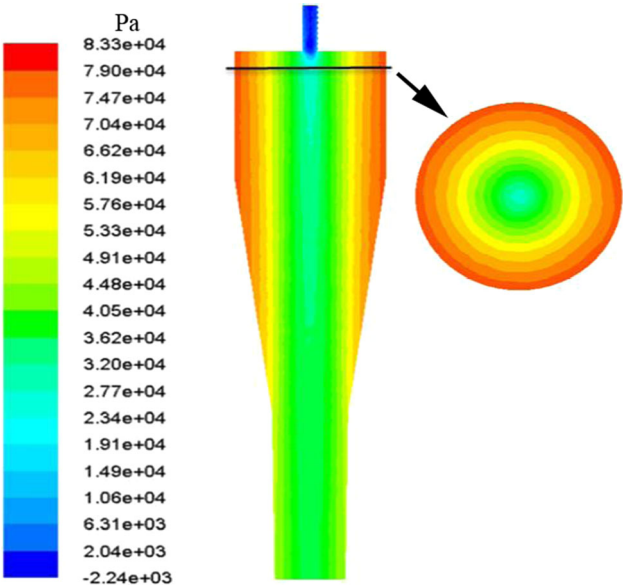

Fig. 5 The pressure variation of the fluid flow in the inner part of the cyclone

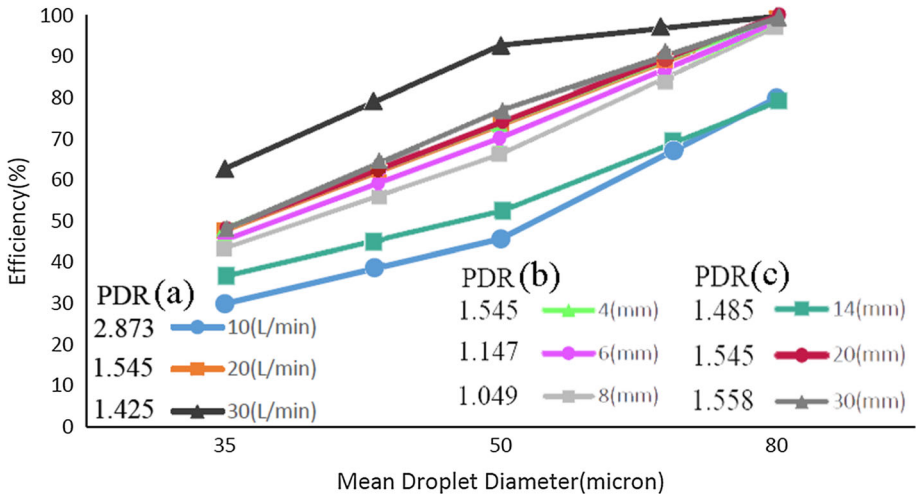

Fig. 6 Comparing the separation efficiencies and pressure drop ratio of the hydro-cyclone with different **a** inlet flowrates, **b** diameters of top offloading pipe and **c** diameters of reducing section

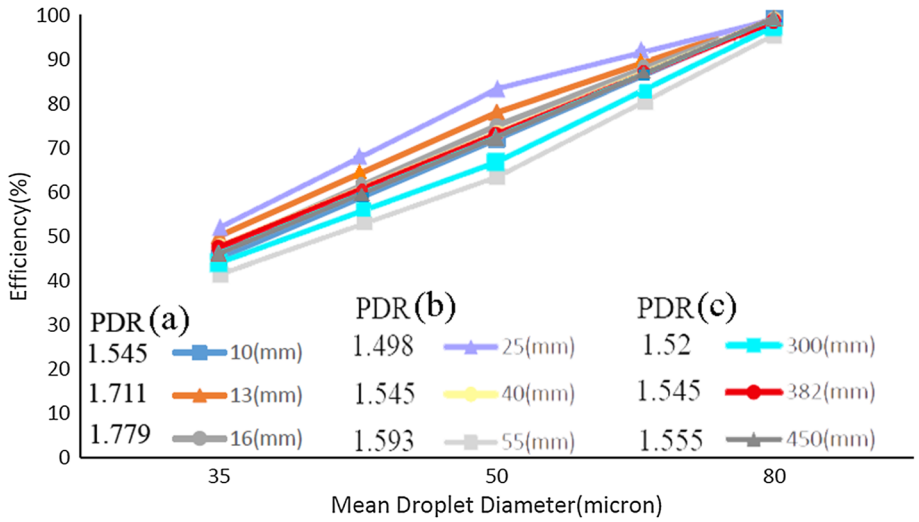

Fig. 7 Comparing the separation efficiencies and pressure drop ratio of the hydro-cyclone with different **a** diameters of tapered section, **b** lengths of cylindrical section and **c** lengths of tapered section

$$\frac{\partial}{\partial t}\left(\rho_m \overrightarrow{v_m}\right) + \nabla.\left(\rho_m \overrightarrow{v_m}\,\overrightarrow{v_m}\right) = -\nabla P + \nabla.\left[\mu_m\left(\nabla \overrightarrow{v_m} + \nabla \overrightarrow{v_m^T}\right)\right] + \rho_m \overrightarrow{g} + \overrightarrow{F} + \nabla.\left(\sum_{k=1}^{n} \alpha_k \rho_k \overrightarrow{v_{dr,k}}\,\overrightarrow{v_{dr,k}}\right) \quad (2)$$

where P presents the pressure value, $\overrightarrow{g}$ is the gravitational acceleration vector, $\overrightarrow{F}$ is the vector of external forces and $\mu_m = \sum_{k=1}^{n} \alpha_k \mu_k$ is the viscosity of mixture. $\overrightarrow{v_{dr,k}} = \overrightarrow{v_k} - \overrightarrow{v_m}$ is the drift velocity vector of the kth phase that can be calculated using the relative velocity of p and q phases ($\overrightarrow{v_{pq}} = \overrightarrow{v_p} - \overrightarrow{v_q} = \frac{(\rho_p - \rho_m) d_p^2}{18 \mu_q f_{\text{drag}}} \overrightarrow{a}$) as $\overrightarrow{v_{dr,p}} = \overrightarrow{v_{pq}} - \sum_{k=1}^{n} \frac{\alpha_k \rho_k}{\rho_m} \overrightarrow{v_{qk}}$, where d_p is the droplet diameter, $f_{\text{drag}} = \begin{cases} 1 + 0.15\text{Re}^{0.687} & \text{Re} \le 1000 \\ 0.0183\text{Re} & \text{Re} > 1000 \end{cases}$ is the drag function and $\overrightarrow{a} = \overrightarrow{g} - \left(\overrightarrow{v_m}.\overrightarrow{\nabla}\right)\overrightarrow{v_m} - \frac{\partial \overrightarrow{v_m}}{\partial t}$ is the acceleration vector of droplet. The volume fraction of another phase has been calculated using the following equation [21]:

$$\frac{\partial}{\partial t}\left(\alpha_k \rho_k\right) + \nabla.\left(\alpha_k \rho_k \overrightarrow{v_m}\right) = -\nabla.\left(\alpha_k \rho_k \overrightarrow{v_{dr,k}}\right) \quad (3)$$

The previous studies approved the abilities of the Reynold stress model for an accurate simulation of this turbulent flow inside the hydro-cyclone [7, 22–24]. Therefore, this model has been used for simulating this fluid flow as below [25]:

$$\frac{\partial}{\partial t}\left(\rho\overline{u_i'u_j'}\right)+\frac{\partial}{\partial x_k}\left(\rho u_k\overline{u_i'u_j'}\right)=-\frac{\partial}{\partial x_k}\left[\overline{u_i'u_j'u_k'}+P'\left(\delta_{kj}u_j'+\delta_{ik}u_j'\right)\right]+\frac{\partial}{\partial x_k}\left[\mu_m\frac{\partial}{\partial x_k}\left(\overline{u_i'u_j'}\right)\right]-\rho_m\left(\overline{u_i'u_k'}\frac{\partial u_j}{\partial x_k}+\overline{u_i'u_k'}\frac{\partial u_i}{\partial x_k}\right)+\overline{P'\left(\frac{\partial u_i'}{\partial x_j}+\frac{\partial u_j'}{\partial x_i}\right)}-2\mu_m\overline{\frac{\partial u_i'}{\partial x_j}\frac{\partial u_j'}{\partial x_i}} \quad (4)$$

hence P' and u' are the fluctuations of the pressure and velocity values, and δ is the kronecker delta. The presented governing equations have been solved, numerically, using the QUICK method. The SIMPLE algorithm and PRESTO model have been used for relating the pressure to the velocity and discretization of the pressure in this simulation, respectively. The acceptable accuracy for the convergence of these calculations has been considered as 10^{-5}. Finally, a set of numerical simulations with a full factorial design has been investigated for obtaining the optimum sizes for the reduced section length and diameter and also the length of the cylindrical section.

Results and Discussion

All the presented results in this section have been based on $\text{Efficiency} = \frac{\text{Mass flowrate of outlet oil from top offload}}{\text{Mass flowrate of inlet oil}}$ and $\text{Pressure drop ratio} = \frac{\text{Inlet pressure of top offload}}{\text{Inlet pressure}-\text{Pressure of bottom offload}}$. First, the grid study has been presented to show the mesh independency of this numerical solution. For this purpose, the hydro-cyclone has been meshed with 105,000, 300,000 and 380,000 calculation cells. The results of this study have been presented in Fig. 2. As seen in this figure, 300,000 cells have suitable accuracy and calculation time. Therefore, this mesh was used for this simulation. In the second step, the accuracy of the developed model is validated with the experimental data of Belaidi and Thew [26] study for validating the accuracy of these predictions. Figure 2 shows this comparison, and this comparison approves the ability of this model to simulate this fluid flow.

The entered pressure on the oil in the radial direction, which has been provided by the vortex flow inside the hydro-cyclone (as seen in Fig. 3), causes the motions of the oil and water phases toward the center and wall of the hydro-cyclone, respectively. Figure 4 shows this phenomenon inside the cyclone. Figure 5 shows the pressure variations within the hydro-cyclone. The formed vortex flow by the tangential fluid inlet provided radial and axial pressure gradients. It is clear that the fluid pressure value close to the cyclone walls is more than its center-line. A

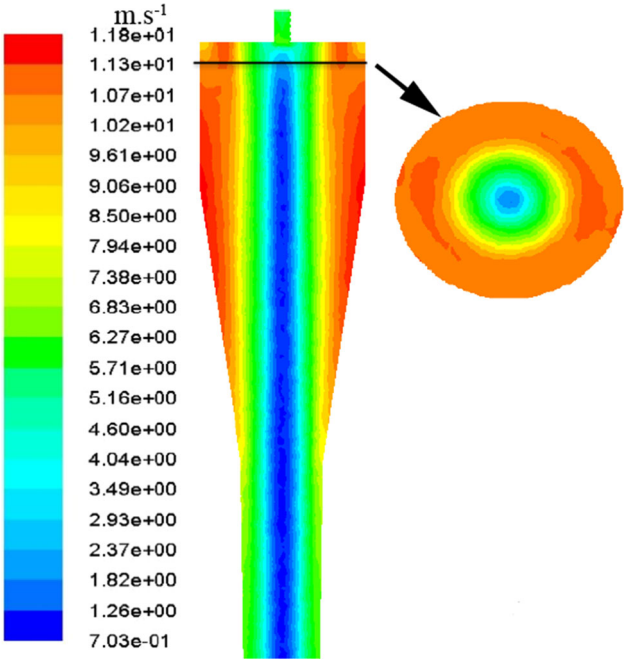

Fig. 9 Effects of hydrophobic wall of the cyclone on the fluid velocity profiles

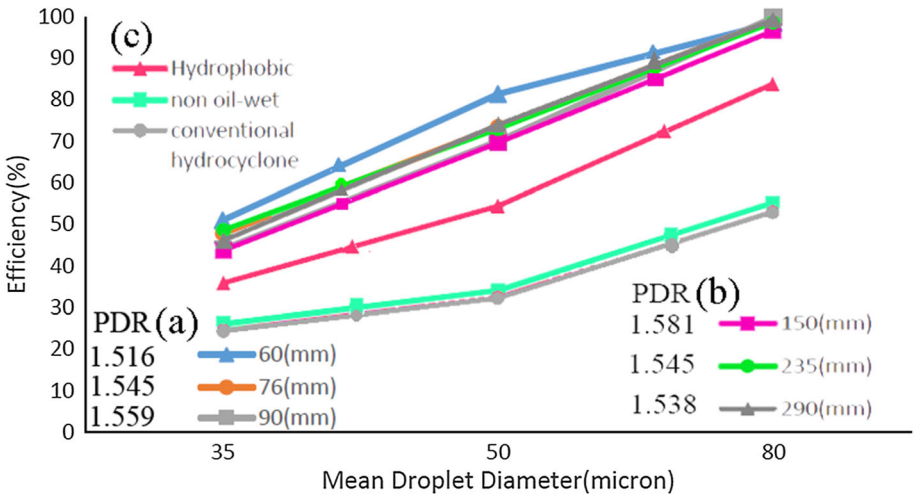

Fig. 8 Comparing the separation efficiencies and pressure drop ratio of the hydro-cyclone with different **a** lengths of reducing section and **b** lengths of the tail pipe, and also **c** effects of hydrophobic and oleophobic walls of the cyclone on its separation efficiency

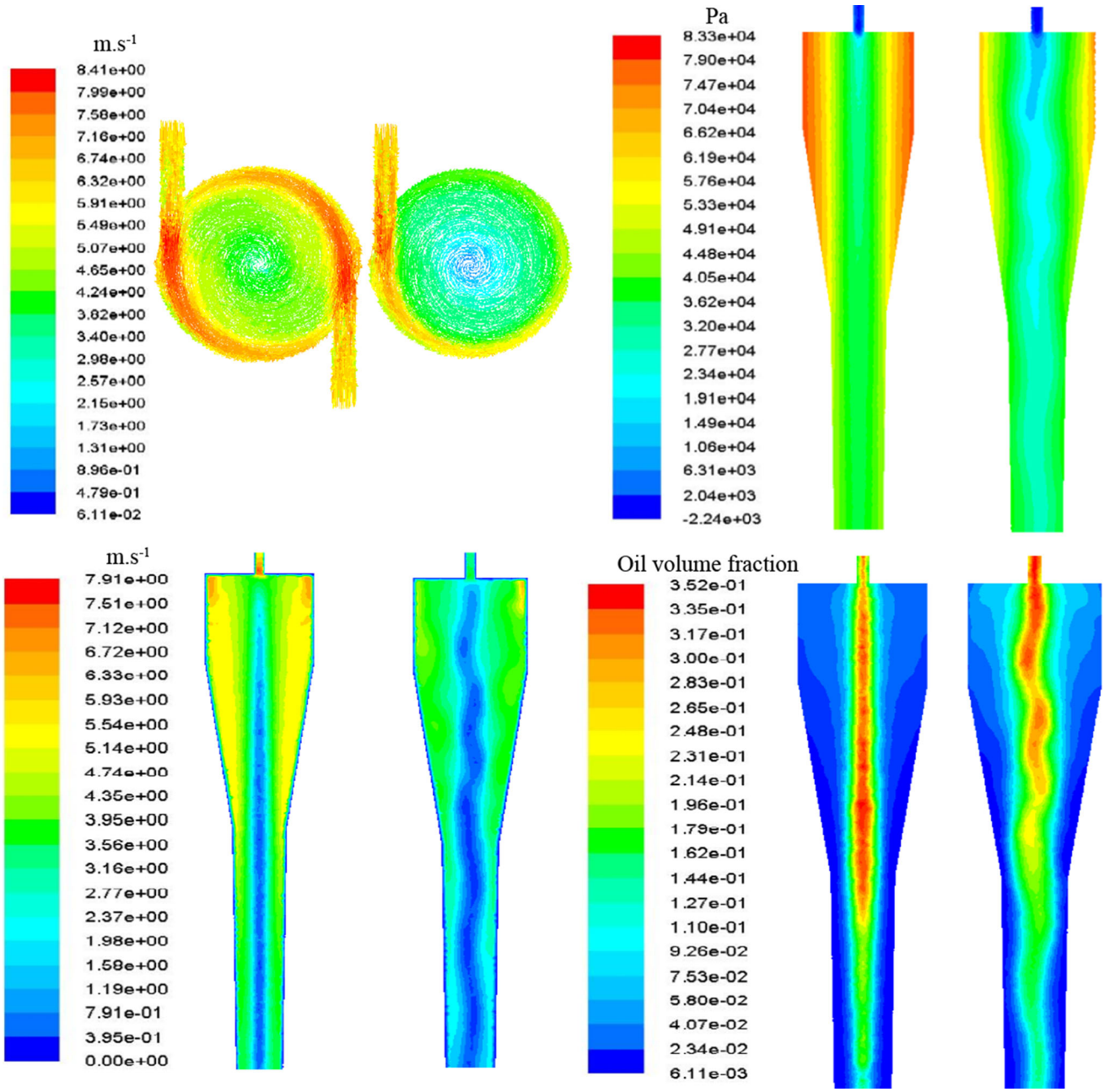

Fig. 10 Effects of the number of inlet pipes of the hydro-cyclone on its performance

vacuum zone is near the top offloading zone, which caused the upward fluid flow inside the cyclone.

Figure 6a compares the separation efficiency of the hydro-cyclone with different inlet flowrates. It is clear that increasing this flowrate improves the efficiency of this cyclone. The oil separation in the tapered section has been resulted from the entered circulation force on the oil droplets in its residence time. This force has been provided by a suitable entrance flow of the mixture fluid. High flowrates of inlet fluid flow improve the vortex flow inside the cyclone and increase the oil separation rate from the water, consequently. This figure also presents the pressure drop ratios (PDR) for different inlet flowrates. It is clear that increasing this flowrate decreases this ratio.

Figure 6b compares the separation efficiencies and also pressure drop ratio of the hydro-cyclone with different diameters of top offloading pipe. It is observed that increasing this diameter ameliorates the cyclone separation efficiency and decreases the pressure drop ratio in this cyclone. Figure 6c compares the separation efficiencies and also pressure drop ratio of the hydro-cyclone with different diameters of reducing section. It is clear that increasing this diameter increases the residence time of mixture inside the hydro-cyclone with a suitable vortex velocity, increases the

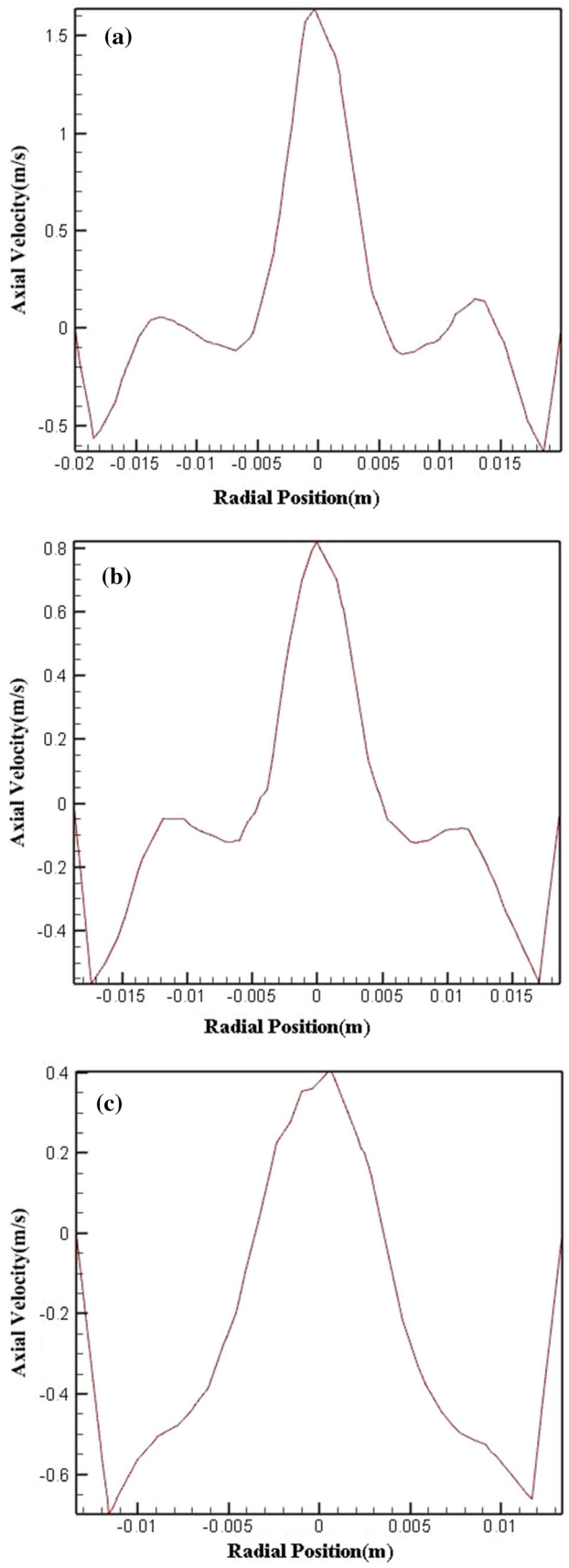

◀**Fig. 11** Axial velocities at **a** 10, **b** 50 and **c** 90 mm from the top part of the hydro-cyclone

separation efficiency of the cyclone and increases its pressure drop ratio, consequently. Figure 7a compares the separation efficiencies and also pressure drop ratio of the hydro-cyclone with different diameters of tapered section. Increasing the size of this section increases the residence time of mixture fluid inside this section of cyclone with a suitable centrifugal force. But, increasing the diameter of this section decays the vortex velocity of the fluid; therefore, this increment decreases the oil separation of this hydro-cyclone. This increment also increases the pressure drop ratio of the cyclone.

Figure 7b compares the separation efficiencies and also pressure drop ratio of the hydro-cyclone with different lengths of cylindrical section. Increasing the length of this section of hydro-cyclone increments the residence time of the mixture fluid inside the section of cyclone with a low vortex velocity. In addition, increasing the length of this section of cyclone increases the entered force from the wall side to the fluid, decreases the vortex flow velocity and decays the separation efficiency of the cyclone and also increases its pressure drop ratio, consequently. Figure 7c compares the separation efficiencies and also pressure drop ratio of the hydro-cyclone with different lengths of tapered section. Increasing this length increases the residence time of the mixture fluid inside this section of the cyclone that has a suitable vortex velocity for this separation. However, increasing this length also increases the entered force from the cyclone wall to the fluid flow and prevents its separation efficiency improvement for too long tapered sections. It is the reason of increasing of the pressure drop ratio of the cyclone with increasing the longitudinal dimension of this section. Figure 8a compares the separation efficiencies and also pressure drop ratio of the hydro-cyclone with different lengths of reducing section. It is clear that increasing the length of this section decays the separation efficiency of the hydro-cyclone. Attending to the slope of the cyclone wall and also high velocity of the fluid flow in this section, this increment increases the extent of the flow turbulence and decays the separation efficiency, as a result. This increment also increases the pressure drop ratio of the cyclone. Figure 8(b) compares the separation efficiencies and also pressure drop ratio for length variation of the tail pipe. Increasing the length of this pipe increases the residence time of the mixture fluid inside the cyclone, but also increases the wall effects that decays the vortex velocity of the fluid flow. These factors have positive and negative effects on the separation efficiency of related cyclone. By

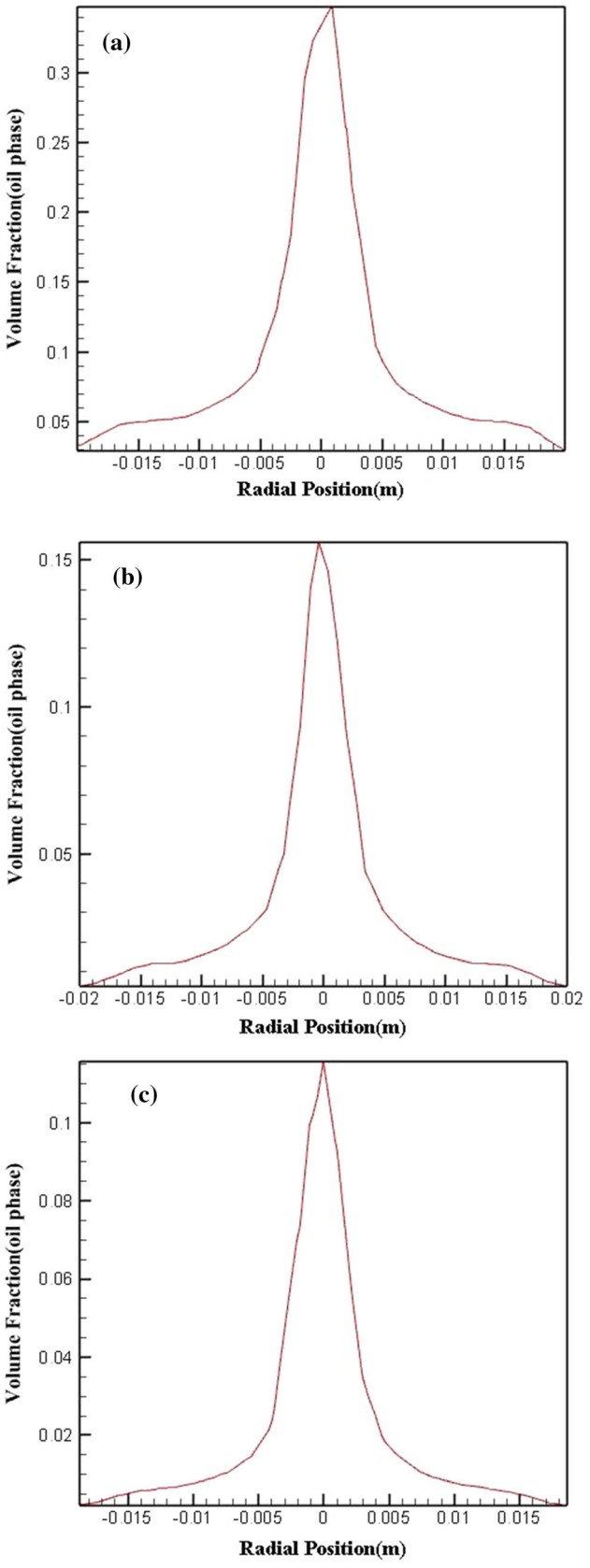

Fig. 12 Volume fractions of the dispersed oil phase within the hydro-cyclone at **a** 10, **b** 50 and **c** 90 mm from top of the hydro-cyclone

Table 1 Obtaining the optimum geometry of the cyclone using a set of numerical simulations

Case	Reducing diameter (mm)	Cylindrical length (mm)	Reducing length (mm)	Efficiency (%)	PDR
1	14	40	90	52.1	1.468
2	20	40	60	78.5	1.524
3	30	40	90	75.7	1.579
4	20	40	76	73	1.545
5	14	40	60	50.7	1.497
6	30	25	90	77.1	1.538
7	20	55	90	60.7	1.605
8	14	55	76	44.2	1.498
9	14	55	90	48.5	1.487
10	30	25	76	77.8	1.515
11	14	25	60	57.1	1.486
12	20	55	76	63.5	1.598
13	20	25	76	80.7	1.509
14	30	55	76	73.5	1.619
15	14	25	90	55	1.466
16	30	25	60	82.1	1.492
17	20	40	90	70	1.594
18	20	25	60	84.2	1.473
19	14	55	60	44.2	1.496
20	20	55	60	67.8	1.588
21	30	40	60	77.8	1.533
22	30	55	90	70	1.641
23	30	40	76	75	1.561
24	20	25	90	79.2	1.515
25	14	40	76	52.1	1.491
26	14	25	76	56.4	1.486
27	30	55	60	75	1.593

increasing the length of this section of the cyclone also, the pressure drop ratio decreases.

Figure 8c shows the effects of hydrophobic and oleophobic walls of the cyclone on its separation efficiency. It is clear that oleophobic wall has no important effect on the cyclone performance, because the oil volume fraction in the mixture fluid is low. Nevertheless, the hydrophobic wall has an important effect on the cyclone separation efficiency improvement. Attending to the slip condition of this type of cyclone wall for the water fluid, this wall has no effects on the vortex flow velocity (see the fluid velocity profiles in Fig. 9). Figure 10 illustrates the effects of the number of inlet pipes of the hydro-cyclone on its performance. It is clear that the symmetry of the flow inside the cyclone with double inlet pipes is more than the cyclone with a single inlet pipe. This symmetry improves the vortex flow inside the cyclone and improves its separation ratio, consequently.

Figure 11 demonstrates the axial direction of the fluid velocities in three various heights of the hydro-cyclone. The results investigated that, near the wall, the fluid velocity is negative, which means that flow is downward, and at the axial location of the hydro-cyclone, the fluid velocity is positive, indicating the reverse flow (upward flow) at this axis. The junction of these two fluid flows with opposite directions is known as the zero vertical velocity (LZV). Drops in this area have an equal chance for entering to the upstream (reverse flow) or downstream flow. The results show that, from the upside to the bottom part of the hydro-cyclone, the reverse flow has been decreased and the downward flow has been increased. Figure 12 illustrates the volume fractions of the dispersed oil phase within the hydro-cyclone at different heights of the hydro-cyclone. It is clear that, from the top to the downward part of the hydro-cyclone, the volume fraction of the dispersed phase has been decreased, which confirms the existence of the reverse flow.

As previously described, a full fractional factorial design of numerical runs has been developed for obtaining the optimum sizes of the most important dimensions of the hydro-cyclone geometry. Therefore, 27 cases of hydro-cyclone with different length dimension of the cylindrical section and the length and diameter of the reducing segment have been simulated and the predicted values of the separation efficiency and also the pressure drop ratio of the cyclone have been compared. Table 1 presents the obtained values for these target parameters in these cases. Considering the presented values in this table, the optimum values for the cylindrical section length and the length and diameter of the reducing section are 25, 60 and 20 mm, respectively. The obtained optimum design for this cyclone has 84.2% separation efficiency.

Conclusions

In this study, a three-dimensional simulation of the oil–water two-phase mixture fluid separation in a hydro-cyclone has been presented. The mixture model and also the Reynold stress model were used for this modeling. After the grid study in order to show independency of grid and validation of the presented model with experimental results, effects of various geometrical and operational parameters on the cyclone performance were investigated. Finally, an optimum design with high separation efficiency was presented. The following conclusions were obtained in the present study:

- Increasing the inlet flowrate of the mixture fluid enhances the separation efficiency factor and reduced the pressure drop ratio of the cyclone.
- Increasing the top offloading pipe decreases the separation efficiency and also the pressure drop ratio of the cyclone.
- Increasing the diameter of the reducing section increments the separation efficiency and additionally the pressure drop ratio of the cyclone.
- Increasing the diameter of the tapered section increases the separation efficiency and also the pressure drop ratio of the cyclone.
- By increasing the length of the cylindrical section, the separation efficiency and the pressure drop ratio of the cyclone decreases and increases, respectively.
- Increasing the axial dimension of the tapered section increases the separation efficiency and additionally the pressure drop ratio of the cyclone.
- Increasing the length of the reducing section decreases the separation efficiency and increases the pressure drop ratio of the cyclone.
- Increasing the length of the tail pipe increases the separation efficiency and decreases the pressure drop ratio of the cyclone.
- A double inlet cyclone has a more separation efficiency than a single inlet cyclone.
- A hydrophobic wall improves the separation efficiency of the hydro-cyclone.
- The optimum sizes for the length of the cylindrical section and the length and diameter of the reducing section are 25, 60 and 20 mm, respectively.

Conflict of interest There is no conflict of interest.

References

1. C. Gomez, J. Caldentey, S. Wang, L. Gomez, R. Mohan, O. Shoham, Oil/water separation in liquid/liquid hydrocyclones (LLHC): part 1 experimental investigation. SPE J. **7**, 353–372 (2002)
2. S. Noroozi, S.H. Hashemabadi, CFD simulation of inlet design effect on deoiling hydrocyclone separation efficiency. Chem Eng Technol Ind Chem Plant Equip Process Eng Biotechnol **32**, 1885–1893 (2009)
3. A. Motin, *Theoretical and Numerical Study of Swirling Flow Separation Devices for Oil-Water Mixtures* (Michigan State University, Michigan, 2015).
4. K. Heiskanen, *Particle Classification* (Chapman & Hall, London, 1993).
5. C. Gomez, J. Caldentey, S. Wang, L. Gomez, R. Mohan, O. Shoham, Oilwater separation in liquid-liquid hydrocyclones (LLHC)-experiment and modeling, in SPE Annual Technical Conference and Exhibition, 2001.
6. G. Young, W. Wakley, D. Taggart, S. Andrews, J. Worrell, Oil-water separation using hydrocyclones: an experimental search for optimum dimensions. J. Petrol. Sci. Eng. **11**, 37–50 (1994)
7. N. Kharoua, L. Khezzar, Z. Nemouchi, CFD simulation of liquid-liquid hydrocyclone: oil/water application. in ASME 2009 Fluids Engineering Division Summer Meeting, 2009, pp. 2085–2094

8. J. Hargreaves, R. Silvester, Computational fluid dynamics applied to the analysis of deoiling hydrocyclone performance. Chem. Eng. Res. Des. **68**, 365–383 (1990)
9. S. Grady, G. Wesson, M. Abdullah, E. Kalu, Prediction of 10-mm hydrocyclone separation efficiency using computational fluid dynamics. Filtr. Sep. **40**, 41–46 (2003)
10. C. Petty, S. Parks, Flow structures within miniature hydrocyclones. Miner. Eng. **17**, 615–624 (2004)
11. S. Huang, Numerical simulation of oil-water hydrocyclone using reynoldsstress model for Eulerian multiphase flows. Can J Chem Eng **83**, 829–834 (2005)
12. Z.S. Bai, H.L. Wang, S.T. Tu, Experimental study of flow patterns in deoiling hydrocyclone. Miner. Eng. **22**, 319–323 (2009)
13. L. Zhao, M. Jiang, F. Li, Experimental study on the separation performance of air-injected de-oil hydrocyclones. Chem. Eng. Res. Des. **88**, 772–778 (2010)
14. T.R. Vakamalla, K.S. Kumbhar, R. Gujjula, N. Mangadoddy, Computational and experimental study of the effect of inclination on hydrocyclone performance. Sep. Purif. Technol. **138**, 104–117 (2014)
15. J. Chen, J. Hou, G. Li, C. Xu, B. Zheng, The effect of pressure parameters of a novel dynamic hydrocyclone on the separation efficiency and split ratio. Sep. Sci. Technol. **50**, 781–787 (2015)
16. H. Osei, H. Al-Kayiem, F. Hashim, Numerical studies on the separation performance of liquid-liquid Hydrocyclone for higher water-cut wells. in IOP Conference Series: Materials Science and Engineering, 2015, p. 2014.
17. X. Fan, "Oil-water separation efficiency and fluid mechanics of a hydrocyclone", 2016.
18. P. Qian, J. Ma, Y. Liu, X. Yang, Y. Zhang, H. Wang, Concentration distribution of droplets in a liquid liquid hydrocyclone and its application. Chem. Eng. Technol. **39**, 953–959 (2016)
19. A. Motin, A. Benard, Design of liquid–liquid separation hydrocyclones using parabolic and hyperbolic swirl chambers for efficiency enhancement. Chem. Eng. Res. Des. **122**, 184–197 (2017)
20. Fluent users guide. Fluent, Inc, 2006.
21. FLUENT.INC Press, Part17: "Mixture model theory."
22. T. Chuah, J. Gimbun, T.S. Choong, A CFD study of the effect of cone dimensions on sampling aerocyclones performance and hydrodynamics. Powder Technol. **162**, 126–132 (2006)
23. W. Griffiths, F. Boysan, Computational fluid dynamics (CFD) and empirical modelling of the performance of a number of cyclone samplers. J. Aerosol Sci. **27**, 281–304 (1996)
24. R. Maddahian, B. Farhanieh, S.D. Saemi, T. Bilstad, Numerical simulation of deoilin hydrocyclones. World Acad. Sci. Eng. Technol. **59**, 2044–2049 (2011)
25. FLUENT.INC Press, Part4: "Turbulence model ".
26. A. Belaidi, M. Thew, The effect of oil and gas content on the controllability and separation in a de-oiling hydrocyclone. Chem. Eng. Res. Des. **81**, 305–314 (2003)
27. J.A. Delgadillo, R.K. Rajamani, Exploration of hydrocyclone designs using computational fluid dynamics. Int. J. Miner. Process. **84**(1–4), 252–261 (2007)
28. M. Narasimha, R. Sripriya, P.K. Banerjee, CFD modelling of hydrocyclone—prediction of cut size. Int. J. Miner. Process. **75**(1–2), 53–68 (2005)
29. J.A. Delgadillo, R.K. Rajamani, A comparative study of three turbulence-closure models for the hydrocyclone problem. Int. J. Miner. Process. **77**(4), 217–230 (2005)
30. N. Chakraborti, J.D. Miller, Fluid flow in hydrocyclones: a critical review. Miner. Process. Extract. Metull. Rev. **11**(4), 211–244 (1992)
31. N. Chakraborti, A. Shekhar, A. Singhal, S. Chakraborty, S. Chowdhury, R. Sripriya, Fluid flow in hydrocyclones optimized through multi-objective genetic algorithms. Inverse Probl. Sci. Eng. **16**(8), 1023–1046 (2008)
32. J.A. Delgadillo, R.K. Rajamani, Hydrocyclone modeling: large eddy simulation CFD approach. Min. Metall. Explor. **22**(4), 225–232 (2005)
33. P.D. Suresh et al., Performance characteristics of pilot plant dense media hydrocyclone for beneficiation of coal and 3-D CFD simulation. Chem. Eng. Sci. **65**(16), 4661–4671 (2010)
34. K.T. Hsieh, R.K. Rajamani, Mathematical model of the hydrocyclone based on physics of fluid flow. AIChE J. **37**(5), 735–746 (1991)
35. T.C. Monredon, K.T. Hsieh, R.K. Rajamani, Fluid flow model of the hydrocyclone: an investigation of device dimensions. Int. J. Miner. Process. **35**(1–2), 65–83 (1992)
36. N Kharoua, L Khezzar, Z Nemouchi, CFD simulation of liquid-liquid hydrocyclone: oil/water application. in Fluids Engineering Division Summer Meeting 2009 Jan 1 (Vol. 43727, pp. 2085–2094).
37. J.C. Cullivan, R.A. Williams, T. Dyakowski, C.R. Cross, New understanding of a hydrocyclone flow field and separation mechanism from computational fluid dynamics. Miner. Eng. **17**(5), 651–660 (2004)